

Topological phases arising from attractive interaction and pair hopping in the Extended Hubbard Model

Roman Rausch*

Department of Physics, Kyoto University, Kyoto 606-8502, Japan

Matthias Peschke†

Department of Physics, University of Hamburg, Jungiusstraße 9, D-20355 Hamburg, Germany

The extended Hubbard model with an attractive density-density interaction, positive pair hopping, or both, is shown to host topological phases, with a doubly degenerate entanglement spectrum and interacting edge spins. When the extended interaction terms combine in a charge-SU(2) symmetric fashion, a novel partially polarized pseudospin phase appears, in which the topological features of the spin degrees of freedom coexist with η -wave superconductivity.

Motivation. Spontaneous symmetry breaking and symmetry-protected topological order (SPTO) constitute two major schemes by which phases of matter can be classified. While the former usually requires interactions, the latter is mainly understood in terms of winding numbers of a noninteracting bandstructure. An interplay between the two can be achieved by adding interactions to a topological bandstructure, which alters the corresponding invariants or the nature of the involved edge states [1, 2]. Another intriguing question is whether SPTO itself can arise from interactions, with the possibility of novel properties beyond noninteracting band topology, as a result of the richness of interacting systems.

The $S = 1$ Haldane spin chain has proven to be a paradigm for an interacting SPTO system, evidenced by a two-fold degenerate eigenvalue spectrum of the reduced density matrix (“entanglement spectrum”), a string order parameter, and entangled $S = 1/2$ spins localized at the edges of an open chain [3–6]. When anisotropy or a transverse field is added to the Hamiltonian, the Haldane phase remains robust in a region of the phase diagram, with the entanglement spectrum still being twofold degenerate, while the string order vanishes [6].

A straightforward way to generate a Haldane state in an $S = 1/2$ system is by coupling pairs of spins to an effective $S = 1$, which can be typically achieved by a ferromagnetic interaction. A spin ladder with ferromagnetic coupling across the rungs, equivalent to a $J_1 - J_2$ chain, hosts a Haldane phase with dimerized spins [7]. An alternating ferromagnetic spin-spin coupling on every second site also leads to a Haldane phase in the Hubbard chain, supplanting the Mott phase [8]. In terms of fermionic models, a Haldane phase is found in the anisotropic $t - J$ model [9] or a 3-leg Hubbard ladder at $2/3$ filling [10].

In this work, we report the existence of novel topological phases in the 1D Hubbard chain extended by an *attractive* density-density coupling and a pair hopping with an *overall positive* coupling constant, which exhibit notable differences from the Haldane phase, as will be explained below.

Model. Our model reads as follows:

$$\begin{aligned}
 H = & -t \sum_{\langle ij \rangle \sigma} \left(c_{i\sigma}^\dagger c_{j\sigma} + H.c. \right) \\
 & + U \sum_i \left[\left(n_{i\uparrow} - \frac{1}{2} \right) \left(n_{i\downarrow} - \frac{1}{2} \right) + \frac{1}{4} \right] \\
 & + V_z/4 \sum_{\langle ij \rangle} (n_i - 1)(n_j - 1) \\
 & - V_{xy}/2 \sum_{\langle ij \rangle} \left(c_{i\uparrow}^\dagger c_{i\downarrow}^\dagger c_{j\downarrow} c_{j\uparrow} + H.c. \right),
 \end{aligned} \tag{1}$$

where $c_{i\sigma}^\dagger$ creates an electron with the spin projection $\sigma = \uparrow, \downarrow$ at site i and $n_{i\sigma} = c_{i\sigma}^\dagger c_{i\sigma}$ is the corresponding density, the total density being $n_i = \sum_\sigma n_{i\sigma}$. The chemical potential is kept fixed in the Hamiltonian, so that the groundstate is mostly found at half filling $N = \sum_i n_i = L$ (with L being the length of a 1D chain) except for some phases (see below). The hopping amplitude $t \equiv 1$ between nearest neighbors (denoted by the angle brackets $\langle ij \rangle$) fixes the energy unit ($\hbar \equiv 1$), U is the on-site Coulomb interaction, V_z the nearest-neighbor Coulomb interaction and V_{xy} the pair-hopping amplitude. Note that all these three terms can be derived from the general interaction term under the assumption of constant matrix elements [11]. Thus, the model studied here can also be seen as a piece of a larger phase diagram of the extended 1D Hubbard model with nearest-neighbor interactions. Our definition of V_z and V_{xy} is slightly different from the usual convention, but natural in terms of the charge-SU(2) symmetry of the model. Namely, defining the pseudospin operators

$$\begin{aligned}
 T_i^+ &= (-1)^i c_{i\downarrow} c_{i\uparrow} \\
 T_i^- &= (-1)^i c_{i\uparrow}^\dagger c_{i\downarrow}^\dagger \\
 T_i^x &= 1/2 (T_i^+ + T_i^-) \\
 T_i^y &= i/2 (T_i^+ - T_i^-) \\
 T_i^z &= 1/2 (n_i - 1)
 \end{aligned} \tag{2}$$

we notice that while spin operators couple \uparrow - and \downarrow -states, pseudospin interactions couple empty $|0\rangle$ and doubly oc-

cupied (“doublon”) sites $|\uparrow\downarrow\rangle$ with the same SU(2) algebra relations [12]. V_z couples only the z components and is analogous to an Ising term, while V_{xy} couples the x - and y -components and introduces doublon hopping. At the charge-SU(2) symmetric line $V_{xy} = V_z = V$, the Hamiltonian can be compactly written using $\mathbf{T}_i = (T_i^x, T_i^y, T_i^z)$ as

$$H = -t \sum_{\langle ij \rangle \sigma} (c_{i\sigma}^\dagger c_{j\sigma} + H.c.) + U/2 \sum_i n_i^h + V \sum_{\langle ij \rangle} \mathbf{T}_i \cdot \mathbf{T}_j, \quad (3)$$

where we have also introduced the holon density $n_i^h = 2n_{i\uparrow}n_{i\downarrow} - n_i + 1$. For $V_{xy} = 0$, the model is known as the extended Hubbard model [13–24], for $V_z = 0$ as the Penson-Kolb-Hubbard model [25–33]. We focus on these two cases (using the shorthands “XY cut” and “Z cut”), as well as on the charge-SU(2) symmetric line (“SU(2) cut”), as well as on the charge-SU(2) symmetric line (“SU(2) cut”). Furthermore, we set $U = 2$, as the intermediate phases of interest vanish for strong U [34]. To solve the model, we mostly use the VUMPS (*variational uniform matrix product states*) framework [35], which works directly in the thermodynamic limit. Our code is equipped to exploit both the spin-SU(2) and the charge-SU(2) of the model, whenever it is appropriate [34]. The nonabelian symmetries are encoded directly into the underlying matrix-product states following the approach in Ref. 36.

Phase diagram. It is helpful to consider the extremes of the phase diagram first. For $V_{xy} = V_z = 0$, we have the Mott phase, a singlet for both the spin $\mathbf{S} = \sum_i \mathbf{S}_i = 0$ (defined as $\mathbf{S}_i = 1/2 \sum_{\sigma\sigma'} c_{i\sigma}^\dagger \boldsymbol{\tau}_{\sigma\sigma'} c_{i\sigma'}$, with the Pauli matrices $\boldsymbol{\tau}$), and the pseudospin $\mathbf{T} = \sum_i \mathbf{T}_i = 0$, with a finite charge gap and zero spin gap. It is marked in red in Fig. 1.

For $|V_{xy}|, |V_z| \gg t, U$ we are dealing with an XXZ model in the charge sector and can draw from the corresponding knowledge [5]: For $|V_{xy}| > |V_z|$ the system is in the quasi-long-range-ordered XY-phase (“T-XY”), with correlations between the xy components of the pseudospin decaying as $\langle T_0^- T_r^+ \rangle \sim r^{-1/2}$, which translates to long-range pairing correlations $\langle c_{0\uparrow}^\dagger c_{0\downarrow}^\dagger c_{r\downarrow} c_{r\uparrow} \rangle \sim (-1)^r r^{-1/2}$, interpreted as η -wave superconductivity [31]. For $|V_z| > |V_{xy}|$, the system is in a symmetry-broken pseudo-ferromagnetic state $\langle T_i^z \rangle = L/2$, with the ground state in the empty ($\langle n_i \rangle = 0$) or fully ($\langle n_i \rangle = 2$) occupied band (which we call “T-Ising”). If half filling is forced, one obtains a phase separation between the two configurations [37], with a domain wall in between. For $|V_z| = |V_{xy}|$, the T-XY and the T-Ising phase mix to form a pseudospin ferromagnet (“T-FM”) with $\langle \mathbf{T} \rangle = L/2$ which spontaneously breaks the charge-SU(2) symmetry and it becomes meaningless to distinguish between the two. The ground state still lies in the empty band, but is now degenerate for all projections $T^z = \sum_i T_i^z$, i.e. for all fillings. Note that sponta-

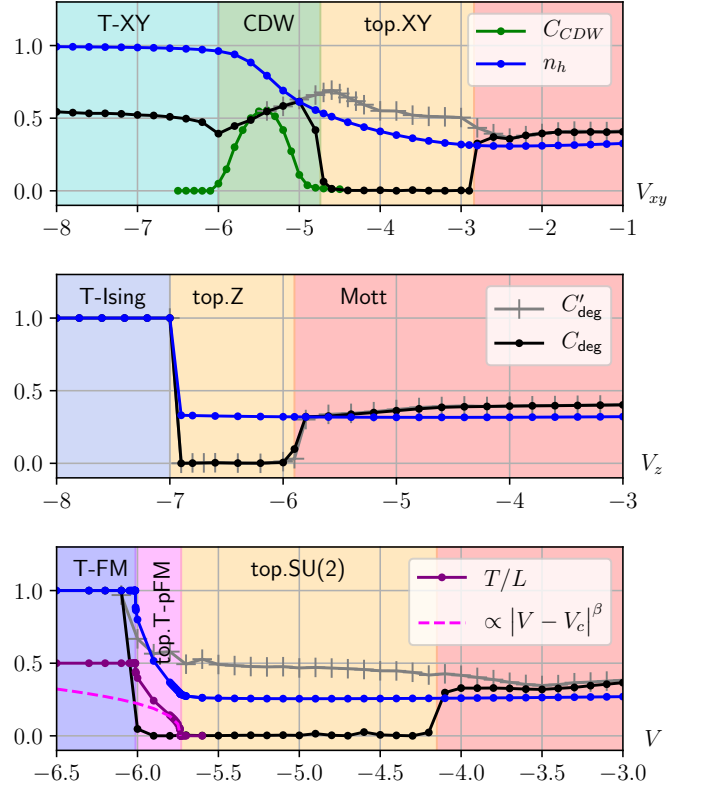


FIG. 1. Phase diagram of the model Eq. (1) for $U = 2$ along the cuts $V_z = 0$ (top), $V_{xy} = 0$ (middle) and $V_{xy} = V_z = V$ (bottom), calculated using VUMPS. Displayed is the degeneracy parameter C_{deg} of the Haldane phase, Eq. (6) (C'_{deg} with broken inversion symmetry, see text), the holon density $n_h = \langle n_i^h \rangle$ (see text), the total pseudospin density T/L , Eq. (5) and the CDW order parameter, Eq. (4). The dotted line is a fit with $|V - V_c|^\beta$ and $\beta \approx 0.351$.

neous symmetry breaking is possible here, even in 1D, because of the absence of quantum fluctuations of \mathbf{T} , since $[H, \mathbf{T}] = 0$.

These three superconducting phases are marked by blue hues in Fig. 1. For the Z cut the transition is first-order, for the XY cut it is continuous, with an intermediate charge density wave (CDW) phase (green in Fig. 1) that breaks translational symmetry and can be identified by looking at the order parameter

$$C_{\text{CDW}} = \frac{1}{2} |\langle n_i \rangle - \langle n_{i+1} \rangle|. \quad (4)$$

For the SU(2) cut, we find that the system first passes through a different intervening phase, a partially polarized pseudospin ferromagnet (“T-pFM”) with the order parameter given by the pseudospin density $0 < T/L < 1/2$, where only a range of fillings around half filling is degenerate [34]. To the best of our knowledge, such a phase has not been reported up to now. We find a second-order transition at $V_{c,1} \approx -5.73$ and $T/L \sim |V - V_c|^\beta$, with $\beta \approx 0.351$, consistent with $\beta = 1/3$. An easy way to ob-

tain this T-pFM phase in a matrix-product state framework is by switching off the charge symmetry altogether (we only exploit the SU(2) spin symmetry), allowing for a superposition of different charge states, and by explicitly calculating

$$T/L = \sqrt{\langle T_i^x \rangle^2 + \langle T_i^y \rangle^2 + \langle T_i^z \rangle^2}. \quad (5)$$

At the transition to the T-FM phase, the calculation then quickly converges to the empty or full band. We find a weakly first-order transition at $V_{c,2} \approx -6.01$ with a small jump in T/L and $\langle n_i^h \rangle$.

We come to the main focus of this paper, two topological phases that are marked yellow in Fig. 1. The main evidence for this comes from the two-fold degeneracy of the eigenvalues s_i of the reduced density matrix $\rho_A = \text{Tr}_B |\Psi\rangle\langle\Psi|$, related to the Schmidt decomposition of the wavefunction into subsystems A and B : $|\Psi\rangle = \sum_i s_i |\Psi_i^A\rangle |\Psi_i^B\rangle$ (for an infinite MPS, this is always a bipartition at a given bond). In Fig. 1, we plot the staggered sum

$$C_{\text{deg}} = \sum_i (-1)^i s_i. \quad (6)$$

This becomes 0 for even degeneracy, 1 for a product state, and can otherwise assume any value in between. We find topological phases with $C_{\text{deg}} = 0$ along each of the three cuts and refer to them as “top.XY”, “top.Z” and “top.SU(2)”. The phases along the XY and the SU(2) cut are protected by inversion symmetry only, which can be checked by adding a weak breaking term $H' = B_{\text{inv}} \sum_{i\sigma} (-1)^i n_{i\sigma}$, $B_{\text{inv}} = 0.01$, that immediately disrupts the full degeneracy. Interestingly, top.Z seems to be protected by more symmetries. According to our computations, it remains robust even if inversion, particle-hole and fermion parity symmetry are broken. Further below, we will also show that the phases are different in terms of correlation functions. Finally, we note that the T-pFM phase also shows $C_{\text{deg}} = 0$, i.e. the system stays topological despite the additional phase transition that leads to superconductivity.

Edge states. To gather further evidence for the topological nature of the phases, we turn to the edge states. Consider the Haldane chain which hosts entangled $S = 1/2$ spins. They interact, forming a singlet and a triplet [4]. This means that the correlation between the first and last site is expected to increase compared with the bulk of the chain [38]. The effective interaction is suppressed with the chain length, so that the singlet-triplet gap vanishes for open boundary conditions in the limit $L \rightarrow \infty$. On the other hand, when there are no edge states, we expect that the correlations between the first site and the rest to simply monotonously decrease with the distance.

We test this effect for the SU(2) cut by calculating the spin-spin correlation between the first spin and the rest,

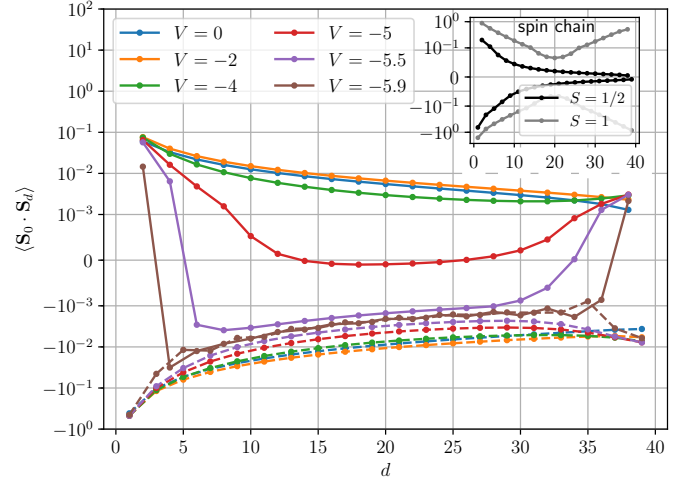


FIG. 2. Spin-spin correlations in an open chain of length $L = 40$ between the first spin and all the others $\langle \mathbf{S}_0 \cdot \mathbf{S}_d \rangle$ ($d = 1 \dots 39$) for $U = 2$ and various values of $V = V_{xy} = V_z$. Inset: Comparison with a spin chain $H = \sum_{\langle ij \rangle} \mathbf{S}_i \cdot \mathbf{S}_j$ for $S = 1/2$ and $S = 1$. Expected phases: $V = 0, -2, -4$: Mott, $V = -5, -5.5$: top.SU(2), $V = -5.9$: top.T-pFM. Even and odd distances are connected by separate lines as a guide for the eyes.

displayed in Fig. 2 for $L = 40$ sites. An analogous behavior is found for the other cuts [34]. The inset compares the nontopological $S = 1/2$ spin chain and the topological $S = 1$ case. The correlation decays with d in the former case, but has a notable uptick coming close to the opposite edge $d \rightarrow L - 1$. The same behaviour is found in our fermionic model: While the correlation is clearly monotonically decreasing for $V = 0$ and $V = -2$, around $V \approx -4$ a notable uptick starts to develop. Furthermore, the qualitative behavior shows a crossover from a staggered pattern to mostly antiferromagnetic correlations.

Gaps and excitations. We have checked both the singlet-triplet gap $\Delta_{S1} = E_0(S = 1) - E_0(S = 0)$ and the singlet-quintet gap $\Delta_{S2} = E_0(S = 2) - E_0(S = 0)$ for open boundary conditions and various system sizes and conclude that they both vanish when extrapolated for $L \rightarrow \infty$ [34]. Assuming that the $S = 2$ excitations lie in the continuum, this indicates gapless bulk states and is a deviation from what is found in the Haldane chain. To better understand this, we look at the dynamics of the bulk system by calculating the spectral function with infinite boundary conditions [39]. It is natural to look both at spin excitations

$$A_S(k, \omega) = \langle 0 | \mathbf{S}_{k\sigma} \delta(\omega + E_0 - H) \mathbf{S}_{k\sigma} | 0 \rangle \quad (7)$$

and at pseudospin excitations given by

$$A_T(k, \omega) = \langle 0 | \mathbf{T}_{k\sigma} \delta(\omega + E_0 - H) \mathbf{T}_{k\sigma} | 0 \rangle, \quad (8)$$

using the Fourier transform $O_k = 1/\sqrt{L} \sum_i \exp(-ikR_i) O_i$ with $O_i = \mathbf{S}_i, \mathbf{T}_i$. In the

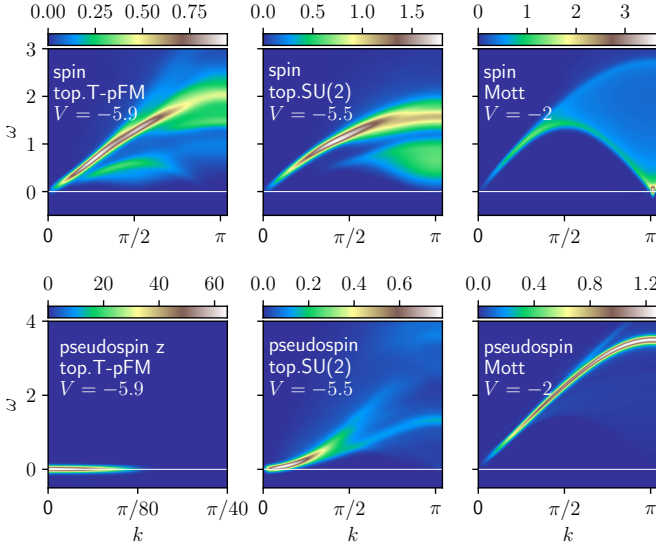


FIG. 3. Dynamical spin and pseudospin structure factor at the charge-SU(2) invariant line, for $U = 2$, values of V and phases as indicated. The pseudospin is approximately half-polarized $T/L \approx 0.24$ in the T-pFM phase. The spin structure factor is according to Eq. (7), while the pseudospin structure factor is according to Eq. (8), except for the T-pFM phase, where charge-SU(2) is broken and we use only the z -component. Additional parameters: infinite boundary conditions with a heterogenous section of length $L = 160$, maximal propagation time $t_{\max} = 48$ inverse hoppings.

T-pFM phase, the charge-SU(2) symmetry is reduced to U(1), and we have to look at the individual components, e.g. $O_i = T_i^z$.

The result is displayed for the SU(2) cut in Fig. 6. One observes that there is in fact a small gap at $k = \pi$ in the topological phase. At $k = 0$, the spin excitations seem to be gapless, but show a kind of pseudogap behavior, with the spectral weight going to zero for $\omega \rightarrow 0$. These features appear to be enough to protect the topology. The same behavior is found for the other two cuts [34].

Looking at the pseudospin excitations, one observes that they are slightly gapped in the Mott phase for $V = -2$, while the gap has closed at $V = -5.5$. At $V = -5.9$, the pseudospin is polarized and we obtain an intense (pseudo-)ferromagnetic peak at $k = 0$, $\omega = 0$. Thus, the topological features in the spin degrees of freedom can coexist with various charge orders in this system.

Correlation functions. In Fig. 4 we show correlation functions at selected points within the various phases. Curiously, the topological phases are characterized by short-range AFM correlations up to a certain length and all-negative correlations beyond that. We find that as $|V_{xy}|$ or $|V_z|$ are increased, the antiferromagnetic range shrinks, and correspondingly the gap at $k = \pi$ of the spin-spin spectral function increases. However, the phases are different in their charge properties: In

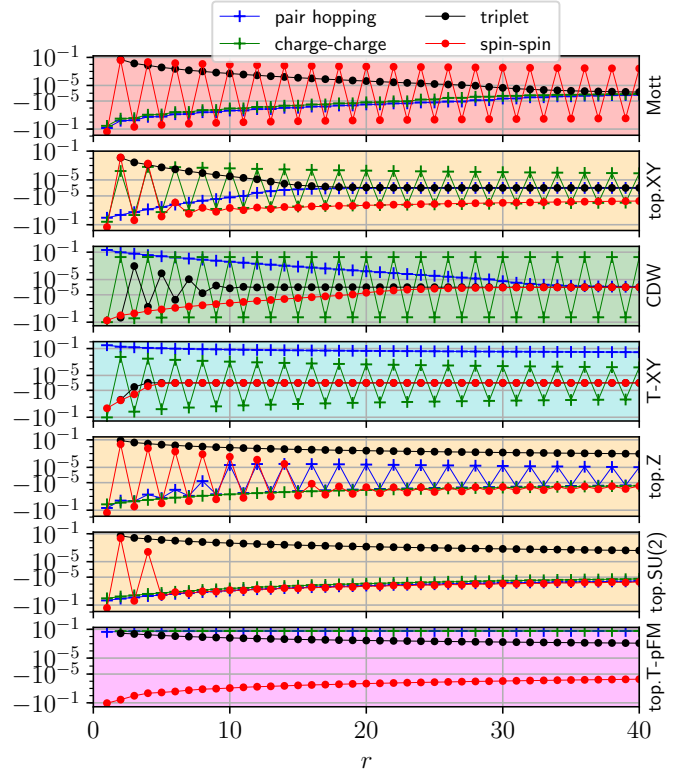


FIG. 4. Correlation functions for selected points in the various phases of Fig. 1. Mott: $V_{xy} = V_z = 0$; top.XY: $V_{xy} = -3.6$, $V_z = 0$; CDW: $V_{xy} = -5.4$, $V_z = 0$; T-XY: $V_{xy} = -7$, $V_z = 0$; top.Z: $V_{xy} = 0$, $V_z = -6.9$; top.SU(2): $V = -5.5$; top.T-pFM: $V = -5.9$. The correlation functions are: pair hopping: $1/2 (\langle T_0^+ T_r^- \rangle + \langle T_0^- T_r^+ \rangle)$, charge-charge: $\langle T_0^z T_r^z \rangle$; triplet-triplet: $\langle \tau_0^i \tau_r^i \rangle$ with $\tau_r = c_{r\uparrow} c_{r+1,\downarrow} + c_{r\downarrow} c_{r+1,\uparrow}$; spin-spin: $\langle \mathbf{S}_0 \cdot \mathbf{S}_r \rangle$. In the charge-SU(2)-invariant phases, pair-hopping and charge-charge correlations are replaced by $\langle \mathbf{T}_0 \cdot \mathbf{T}_r \rangle$.

the top.XY phase we find a staggered quasi-long-range order in the charge-charge correlations (a precursor of the eventual CDW), but decaying triplet and pair hopping correlations, while the top.Z and top.SU(2) phases show quasi-long range order in the latter two. As soon as the spin-spin correlations turn all negative, there is a transition to a long-range ordered state, which is nontopological CDW in the case of the XY cut, but topological T-pFM in the case of the SU(2) cut.

Conclusions. We have shown that the Hubbard chain with attractive density-density interaction and/or positive pair-hopping hosts topological phases, evidenced by even degeneracy of the entanglement spectrum and interacting edge modes. Even though the spin gap remains zero (unlike in the Haldane phase), we find a small gap for $k = \pi$ and vanishing spectral weight for $k \rightarrow 0$. While the phases for $V_z = 0$ and for $V_z = V_{xy} = V$ are protected by reflection symmetry only, we could not yet establish the full set of protecting symmetries for $V_{xy} = 0$. How-

ever, we have checked that the topological properties remain even if inversion, particle-hole and fermion parity symmetry are broken. A complete analysis in terms of symmetries is beyond the scope of this work and is left to future investigations. Interestingly, all phases are marked by AFM spin-spin correlations up to a certain distance, and all-negative correlations beyond that. In the T-pFM phase, these features coexist with long-range η -wave superconductivity (partial pseudospin polarization).

We thank Norio Kawakami and Michael Potthoff for helpful discussions. R.R. thanks the Japan Society for the Promotion of Science (JSPS) and the Alexander von Humboldt Foundation. Computations were partially performed at the Yukawa Institute for Theoretical Physics, Kyoto; partially at the ISSP computation cluster in the University of Tokyo; and partially at the PhysNet computation cluster at Hamburg University. R.R. gratefully acknowledges support by JSPS, KAKENHI Grant No. JP18F18750.

* rausch.roman.72e@st.kyoto-u.ac.jp

† mpeschke@physnet.uni-hamburg.de

- [1] L. Fidkowski and A. Kitaev, *Phys. Rev. B* **81**, 134509 (2010).
- [2] T. Yoshida, R. Peters, S. Fujimoto, and N. Kawakami, *Phys. Rev. Lett.* **112**, 196404 (2014).
- [3] F. Haldane, *Physics Letters A* **93**, 464 (1983).
- [4] T. Kennedy, *Journal of Physics: Condensed Matter* **2**, 5737 (1990).
- [5] H.-J. Mikeska and A. K. Kolezhuk, in *Quantum magnetism* (Springer, 2004) pp. 1–83.
- [6] F. Pollmann, A. M. Turner, E. Berg, and M. Oshikawa, *Phys. Rev. B* **81**, 064439 (2010).
- [7] C. E. Agrapides, S.-L. Drechsler, J. van den Brink, and S. Nishimoto, in *spin*, Vol. 1 (2019) p. 2.
- [8] F. Lange, S. Ejima, and H. Fehske, *Phys. Rev. B* **92**, 041120 (2015).
- [9] S. Fazzini, L. Barbiero, and A. Montorsi, *Phys. Rev. Lett.* **122**, 106402 (2019).
- [10] H. L. Nourse, I. P. McCulloch, C. Janani, and B. J. Powell, *Phys. Rev. B* **94**, 214418 (2016).
- [11] R. Strack and D. Vollhardt, *Phys. Rev. Lett.* **72**, 3425 (1994).
- [12] F. H. Essler, H. Frahm, F. Göhmann, A. Klümper, and V. E. Korepin, *The one-dimensional Hubbard model* (Cambridge University Press, 2005).
- [13] M. Nakamura, *Journal of the Physical Society of Japan* **68**, 3123 (1999).
- [14] M. Vojta, R. E. Hetzel, and R. M. Noack, *Phys. Rev. B* **60**, R8417 (1999).
- [15] M. Nakamura, *Phys. Rev. B* **61**, 16377 (2000).
- [16] H. Lin, D. Campbell, and R. Clay, *Chinese Journal of Physics* **38**, 1 (2000).
- [17] P. Sengupta, A. W. Sandvik, and D. K. Campbell, *Phys. Rev. B* **65**, 155113 (2002).
- [18] M. Tsuchiizu and A. Furusaki, *Phys. Rev. Lett.* **88**, 056402 (2002).
- [19] E. Jeckelmann, *Phys. Rev. Lett.* **89**, 236401 (2002).
- [20] A. W. Sandvik, L. Balents, and D. K. Campbell, *Phys. Rev. Lett.* **92**, 236401 (2004).
- [21] S. Ejima and S. Nishimoto, *Phys. Rev. Lett.* **99**, 216403 (2007).
- [22] M. Kumar, S. Ramasesha, and Z. G. Soos, *Phys. Rev. B* **79**, 035102 (2009).
- [23] D. Sénéchal, A. G. R. Day, V. Bouliane, and A.-M. S. Tremblay, *Phys. Rev. B* **87**, 075123 (2013).
- [24] A. Kantian, M. Dolfi, M. Troyer, and T. Giamarchi, arXiv preprint arXiv:1903.12184 (2019).
- [25] K. A. Penson and M. Kolb, *Phys. Rev. B* **33**, 1663 (1986).
- [26] M. Kolb and K. A. Penson, *Journal of Statistical Physics* **44**, 129 (1986).
- [27] A. Hui and S. Doniach, *Phys. Rev. B* **48**, 2063 (1993).
- [28] B. Bhattacharyya and G. K. Roy, *Journal of Physics: Condensed Matter* **7**, 5537 (1995).
- [29] G. I. Japaridze and E. Müller-Hartmann, *Journal of Physics: Condensed Matter* **9**, 10509 (1997).
- [30] S. Robaszkiewicz and B. R. Bulka, *Phys. Rev. B* **59**, 6430 (1999).
- [31] G. I. Japaridze, A. P. Kampf, M. Sekania, P. Kakashvili, and P. Brune, *Phys. Rev. B* **65**, 014518 (2001).
- [32] G. Japaridze and S. Sarkar, *The European Physical Journal B - Condensed Matter and Complex Systems* **28**, 139 (2002).
- [33] K. J. Kapcia, W. R. Czart, and A. Ptok, *Journal of the Physical Society of Japan* **85**, 044708 (2016), <https://doi.org/10.7566/JPSJ.85.044708>.
- [34] See Supplemental Material at *URL*.
- [35] V. Zauner-Stauber, L. Vanderstraeten, M. T. Fishman, F. Verstraete, and J. Haegeman, *Phys. Rev. B* **97**, 045145 (2018).
- [36] I. P. McCulloch, *Journal of Statistical Mechanics: Theory and Experiment* **2007**, P10014 (2007).
- [37] F. Iemini, T. O. Maciel, and R. O. Vianna, *Phys. Rev. B* **92**, 075423 (2015).
- [38] S. Yamamoto, *Journal of the Physical Society of Japan* **63**, 4327 (1994), <https://doi.org/10.1143/JPSJ.63.4327>.
- [39] H. N. Phien, G. Vidal, and I. P. McCulloch, *Phys. Rev. B* **86**, 245107 (2012).

DETAILS OF THE VUMPS CALCULATION

In our VUMPS algorithm implementation we start with a small bond dimension and increase it dynamically once the variation error and the state error have sufficiently converged. The resulting effective bond dimension χ typically reaches values of $\chi \sim 6.5 \cdot 10^3$ when only spin-SU(2) is exploited (in the T-pFM phase), $\chi \sim 10 \cdot 10^3$ when SU(2) \otimes U(1) is exploited (for $V_{xy} \neq V_z$), and $\chi \sim 20 - 40 \cdot 10^3$ when full SU(2) \otimes SU(2) is exploited (for $V_{xy} = V_z$).

However, to correctly obtain the degeneracies of the eigenvalue spectrum it seems that a certain symmetry breaking is necessary. This can be checked for the simpler case of the $S = 1$ spin chain: When the singular values are resolved by the magnetic quantum number M , the first degenerate pair might be found for $M = 0$ and $M = 1$, the next for $M = -1$ and $M = 2$ and so on, where the exact position is random. While this is easily obtainable in the spin chain, we find it is more difficult for our fermionic model, even though all the correlation functions (which are proper observables) converge. We find that degeneracy in the topological phase is quickly reached either without any symmetries at all or only with one U(1) spin symmetry. Therefore, the degeneracy parameter C_{deg} in the main text is calculated for spin-U(1) only, with a bond dimension of around $\chi \sim 1.2 \cdot 10^3$, while we use the maximal symmetries for all other calculations.

GAPS ALONG THE CHARGE-SU(2) SYMMETRIC LINE

Figure 5 shows several gaps along the charge-SU(2) symmetric line of the model: the charge gap

$$\Delta_C = E_0(S = 1/2, T = 1/2) - E_0(S = 0, T = 0), \quad (9)$$

the pseudospin singlet-triplet gap (corresponding to the addition or removal of two electrons)

$$\Delta_T = E_0(S = 0, T = 1) - E_0(S = 0, T = 0), \quad (10)$$

the spin singlet-triplet gap

$$\Delta_{S1} = E_0(S = 1, T = T_0) - E_0(S = 0, T = T_0), \quad (11)$$

and the singlet-quintet gap (corresponding to two spin-flips)

$$\Delta_{S2} = E_0(S = 2, T = T_0) - E_0(S = 0, T = T_0), \quad (12)$$

where T_0 denotes the pseudospin of the ground state. This is usually $T_0 = 0$ (i.e. half filling), except for the T-pFM phase, where the pseudospin is partially polarized. We observe a vanishing of Δ_{S1} , which could be due to the edge states for open boundary conditions, so that taking Δ_{S2} gap into account is also necessary. Assuming that

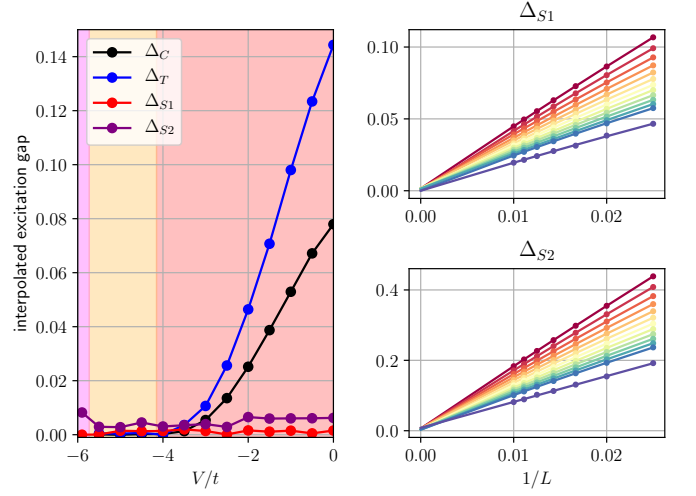


FIG. 5. Gaps of pseudospin (T), charge (C), spin-triplet (S1) and spin-quintet (S2) excitations for open boundary conditions, calculated with DMRG for chain lengths from $L = 40$ to $L = 100$ along the charge-SU(2) invariant line $V_{xy} = V_z = V$. The results are interpolated using a second-degree polynomial of L^{-1} . The insets show the interpolations of Δ_{S1} and Δ_{S2} for (top to bottom) $V = 0, -0.5, -1, \dots, -5, -5.5, -5.9$. The calculation is carried out using SU(2) \otimes SU(2) symmetry, except for $V = -5.9$, where only spin-SU(2) is exploited.

the lowest quintet state lies in the continuum of bulk excited states, we have to conclude that the bulk spin gap must vanish, or at least be very small. Curiously, the topological phase transition around $V \approx -4.1$ is given by the closing of the charge and the pseudospin gap instead. The closing appears to be exponential, consistent with being of Berezinskii-Kosterlitz-Thouless (BKT) type.

SPECTRAL FUNCTION AWAY FROM THE CHARGE-SU(2) SYMMETRIC LINE

Figure 6 shows the spin and pseudospin spectral functions in the topological phase for the XY and for the Z cut, comparing it with the Mott case ($V_{xy} = V_z = 0$). We note that the spin spectral function in the topological phases (center two columns) exhibits the same qualitative behaviour as for the SU(2) cut shown in the main text: The strong antiferromagnetic peak at $k = \pi$ dissolves, leaving a small gap at $k = \pi$ and a pseudogap-like suppression of spectral weight at $k = 0$.

The pseudospin excitations are in both cases gapless, but qualitatively very different: In the top.Z phase, the low-energy excitations are similar to the Mott phase, but gapless, though with vanishing weight for $\omega \rightarrow 0$. In the top.XY phase, they show a (pseudo-)antiferromagnetic behavior with a strong gapless peak at $k = \pi$, corresponding to quasi-long-range order in the static charge-charge correlation shown in the main text. This is due to $V_{xy} < 0$ being equivalent to a repulsive doublon-

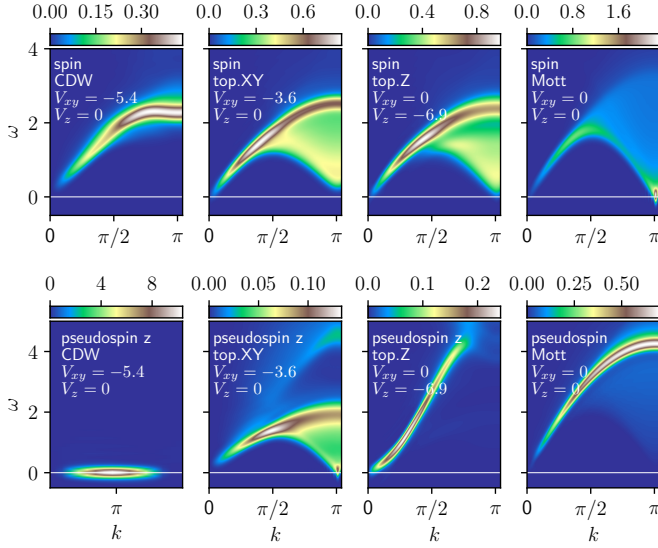


FIG. 6. Dynamical spin and pseudospin structure factor (only the z component where indicated) for the parameters and phases as shown. Additional parameters: infinite boundary conditions with a heterogenous section of length $L = 160$, maximal propagation time $t_{\max} = 24$ inverse hoppings.

doublon interaction, favoring configurations with alternating empty and doubly occupied sites. As $|V_{xy}|$ is increased further ($V_{xy} = -5.4$), it leads to a CDW phase, i.e. a true long-range ordering in the T^z component that shows up as an intense peak at $k = \pi$, $\omega = 0$; and eventually to η -wave superconductivity of doublons (not shown).

EDGE SPIN CORRELATIONS AWAY FROM THE CHARGE-SU(2) SYMMETRIC LINE

Figure 7 shows the correlation between the first spin of an open chain and the rest for the XY cut. Just as for the SU(2) cut presented in the main text, one observes an uptick of the correlation with the last site, clearly visible for $V_{xy} = -3.5, -4, -4.5$, which is consistent with the position of the topological phase, whose limits were obtained from the two-fold degeneracy of the entanglement spectrum using VUMPS. The correlations decrease monotonously for $V_{xy} = -1, -2$ in the Mott phase and exponentially go to zero for $V_{xy} = -5.5$ in the spin-gapped CDW phase.

Figure 8 shows the same for the Z cut, where the uptick is visible for $V_z = -6.5, -6.8$, again consistent with the phase diagram, though the behavior seems somewhat more shallow in this case. One needs to go very deep into the phase (close to the critical $V_z \approx -7$) to see it.

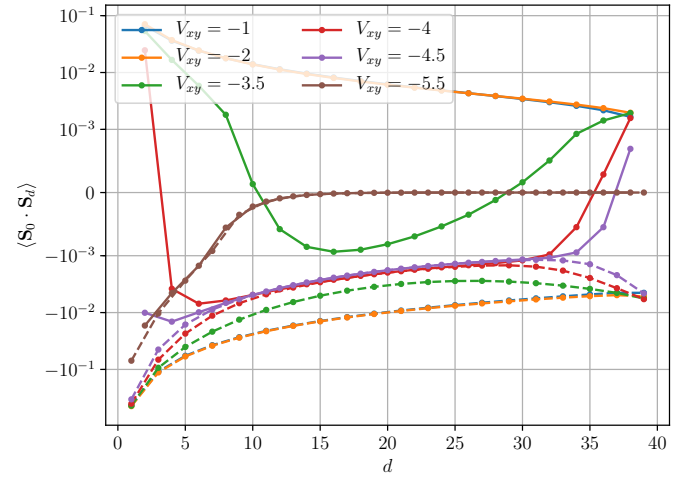


FIG. 7. Spin-spin correlations in an open chain of length $L = 40$ between the first spin and all the others $\langle \mathbf{S}_0 \cdot \mathbf{S}_d \rangle$ ($d = 1 \dots 39$) for $U = 2$, $V_z = 0$ and various values of V_{xy} . Expected phases: $V_{xy} = -1, -2$: Mott, $V_{xy} = -3.5, -4, -4.5$: top.XY, $V_{xy} = -5.5$: CDW. Even and odd distances are connected by separate lines as a guide for the eyes.

EDGE MODE CORRELATIONS IN THE KITAEV CHAIN

To further demonstrate that the method of calculating correlations across the chain reveals the edge states, we briefly compare to the Kitaev chain, given by the following Hamiltonian of spinless fermions:

$$H = -t \sum_{\langle ij \rangle} (c_i^\dagger c_j + H.c.) - \Delta \sum_{\langle ij \rangle} (c_i c_j + H.c.) - \mu \sum_i c_i^\dagger c_i. \quad (13)$$

For $t = \Delta = 1$, there is a topological phase with localized Majorana edge modes for the value range of the chemical potential $|\mu| < 2$. The correlations $\langle c_0^\dagger c_d \rangle$ within the trivial and the topological phase are shown in Fig. 9. At $\mu = \mu_c = -2$, the gap closes and one obtains long-range behavior, for $|\mu| < 2$ there is a sizeable enhancement of the correlation towards the opposite edge. Note that deep in the topological phase ($\mu = 0$), the correlation with the bulk drops to zero and rises again to the same value (in absolute terms) as for the nearest neighbor, while closer to the phase transition ($\mu = -1.8$), it only drops to a small value for the bulk and does not increase as much. The latter behavior is also found in our interacting model: Presumably, once the system is in the topological phase, a further increase of parameters enhances fluctuations that already drive it into the next phase, so that the uptick behavior of the correlation is not as pronounced.

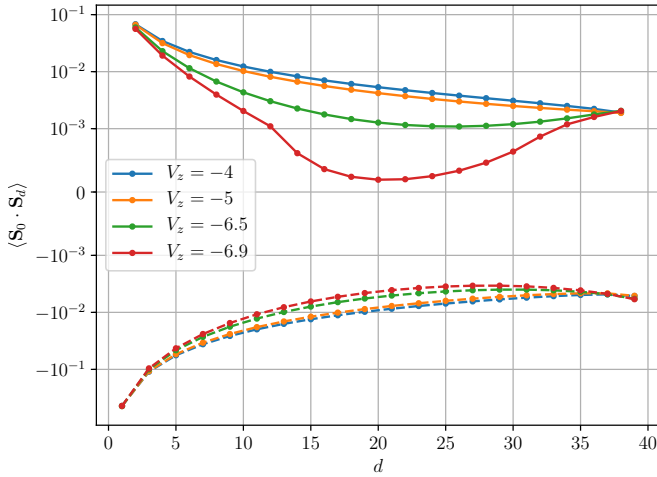


FIG. 8. Same as Fig. 7, but for $V_{xy} = 0$ and various values of V_z . Expected phases: $V_z = -4, -5$: Mott, $V_z = -6, -6.5$: top.Z. Even and odd distances are connected by separate lines as a guide for the eyes.

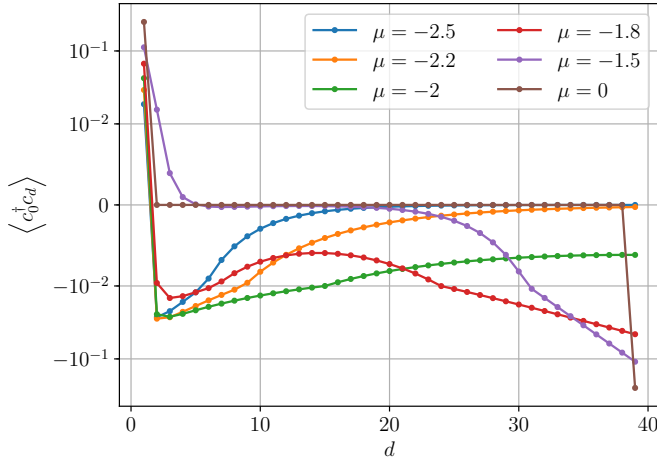


FIG. 9. Hopping correlation between the first site and all the others $\langle c_0^\dagger c_d \rangle$ ($d = 1, \dots, 39$), for the Kitaev chain Eq. (13) of length $L = 40$. Parameters: $t = \Delta = 1$, open boundary conditions.

DEGENERACY CLOSE TO HALF FILLING IN THE T-PFM PHASE

Table I shows the ground-state energies for various fillings in the T-pFM phase for $L = 40$ and $V = -5.9$, calculated with $SU(2) \otimes U(1)$ symmetry, about 100 half-sweeps and resulting in relative energy errors of the order of 10^{-11} and an energy variance of the order of 10^{-6} . We see that the energies are near-degenerate, with a differ-

ence only in the 6-th digit down to a filling of $n = 0.6$. A complete degeneracy is expected in the thermodynamic limit.

| N | n | E_0/L |
|-----|------|-----------------|
| 40 | 1.0 | -0.476414030401 |
| 38 | 0.95 | -0.476414055695 |
| 36 | 0.9 | -0.476413996427 |
| 34 | 0.85 | -0.476414195509 |
| 32 | 0.8 | -0.476414371473 |
| 30 | 0.75 | -0.476414592398 |
| 28 | 0.7 | -0.476414883662 |
| 26 | 0.65 | -0.476415182019 |
| 24 | 0.6 | -0.476415338941 |
| 22 | 0.55 | -0.4761883984 |
| 20 | 0.5 | -0.475594057934 |
| 18 | 0.45 | -0.474608009604 |
| 16 | 0.4 | -0.473219622862 |
| 14 | 0.35 | -0.471430829577 |
| 12 | 0.3 | -0.469257993588 |
| 10 | 0.25 | -0.466740570475 |
| 8 | 0.2 | -0.463980580634 |
| 6 | 0.15 | -0.460746176038 |
| 4 | 0.1 | -0.457503252235 |
| 2 | 0.05 | -0.448273305085 |
| 0 | 0.0 | -0.438125 |

TABLE I. Ground-state energies for $L = 40$, $U = 2$, $V = -5.9$, corresponding to a pseudospin polarization of $T/L \approx 0.24$ in the thermodynamic limit.

DIFFERENT VALUES OF THE LOCAL COULOMB INTERACTION U

Figure 10 shows the phase diagram along the $SU(2)$ cut for $U = 4$. We find that the intervening phases disappear and there is just a first-order phase transition to the T-FM phase at $V_c \approx 9.055$. To explain this it is helpful to consider vanishing hopping $t = 0$. In this case, the remaining U -term commutes with the V -term. The former favors a state of pure antiferromagnetic spins with an energy $E = 0$, while the latter favors the empty band (ferromagnetic pseudospins) with an energy of $E = U/2 + V/4$. The two lines cross at $V = -2U$ where a first-order transition takes place due to a level crossing. Thus, the presence of the interesting intervening phases is an effect of non-negligible hopping, i.e. they appear for $t \sim U$ and the corresponding transition lines must end at a critical endpoint U_c .

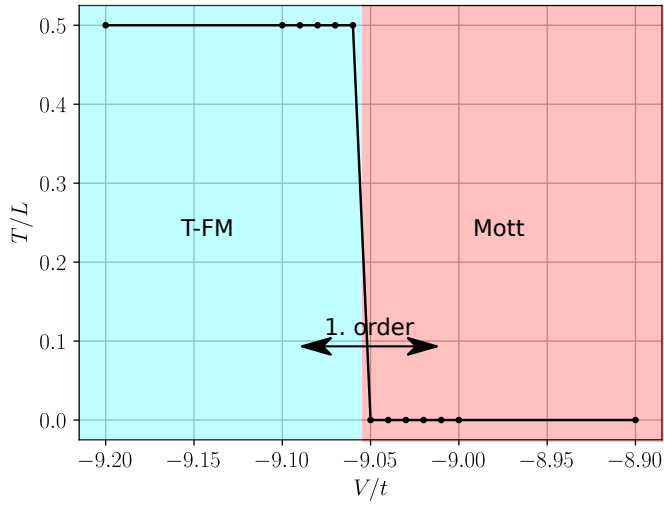


FIG. 10. Phase diagram along the SU(2) cut $V = V_{xy} = V_z$ for $U = 4$ based on the pseudospin density T/L .